

Adaptive Stroud Stochastic Collocation Method for Flow in Random Porous Media via Karhunen-Loève Expansion

Yan Ding¹, Tiejun Li^{1,*}, Dongxiao Zhang^{2,3} and Pingwen Zhang¹

¹ LMAM and School of Mathematical Sciences, Peking University, Beijing 100875, P.R. China.

² Department of Energy and Resources Engineering, College of Engineering, Peking University, Beijing 100871, China.

³ Department of Civil and Environmental Engineering, and Mork Family Department of Chemical Engineering and Materials Science, University of Southern California, Los Angeles, CA 90089, USA.

Received 5 May 2007; Accepted (in revised version) 8 December 2007

Available online 27 February 2008

Abstract. In this paper we develop a Stochastic Collocation Method (SCM) for flow in randomly heterogeneous porous media. At first, the Karhunen-Loève expansion is taken to decompose the log transformed hydraulic conductivity field, which leads to a stochastic PDE that only depends on a finite number of i.i.d. Gaussian random variables. Based on the eigenvalue decay property and a rough error estimate of Stroud cubature in SCM, we propose to subdivide the leading dimensions in the integration space for random variables to increase the accuracy. We refer to this approach as *adaptive Stroud SCM*. One- and two-dimensional steady-state single phase flow examples are simulated with the new method, and comparisons are made with other stochastic methods, namely, the Monte Carlo method, the tensor product SCM, and the quasi-Monte Carlo SCM. The results indicate that the adaptive Stroud SCM is more efficient and the statistical moments of the hydraulic head can be more accurately estimated.

AMS subject classifications: 60H15, 65M70, 76M22, 76S05

Key words: Adaptive Stroud stochastic collocation method, Karhunen-Loève expansion, Monte Carlo simulation, random porous flow.

1 Introduction

Geological formation material properties are ordinarily observed at a few locations although they exhibit a high degree of spatial variability. This leads to uncertainty about

*Corresponding author. *Email addresses:* dyan@math.pku.edu.cn (Y. Ding), tieli@pku.edu.cn (T. Li), donzhang@usc.edu (D. Zhang), pzhang@pku.edu.cn (P. Zhang)

the prediction of subsurface flow. In order to quantify the uncertainty, a stochastic description of the medium properties is needed. This brings the traditional porous medium equations into stochastic partial differential equations (SPDE) [8, 23, 37], which possess more interesting and challenging computational problems.

Monte Carlo (MC) simulation is one of the most natural approaches to solve SPDE. It is a statistical method and the basic idea is to sample a large amount of realizations for the random process and approximate the moments of interest with ensemble average. Thus the number of realizations, which one chooses, controls the accuracy of MC simulation. To ensure the convergence of the moments, typically a few thousand samples or more are required, which is the main disadvantage of the direct sampling MC simulation.

An alternative approach is based on moment equations [10, 13, 20, 37]. This method usually leads to a system of deterministic differential equations which govern the propagation of the statistical moments of the random variables (fields). For deriving these equations, the method of perturbation or some type of closure approximation is needed. However, the computational effort is still high. To compute the hydraulic head covariance to first order in the variability of the log hydraulic conductivity, one needs to solve the deterministic equations for the cross-covariance between the hydraulic head and the log hydraulic conductivity and those for the hydraulic head covariance. If higher-order terms are included, the computational effort will increase dramatically. Zhang et al. recently developed a Karhunen-Loève expansion based moment equation approach (KLME) and applied this method to flows in porous media [5, 6, 17, 35, 38]. With this approach, the equations for the coefficients are uncoupled. One can obtain the high-order terms of the mean and variance of hydraulic head with relatively small computational efforts. The approach can be easily implemented with existing simulators. By these advantages, the KLME approach is generally more efficient than the traditional moment equation approach.

A mathematically unified numerical approach for SPDE — Stochastic Finite Element Method (SFEM) — is also under study and has been rapidly developed in recent years [1, 2, 9, 12, 15]. This method employs the polynomial chaos expansion (PCE) for random processes. After truncation in probability space, its formulation fits into the traditional spectral methods framework, which ensures exponential convergence in probability space [1, 12, 31–33]. However, as the deterministic spectral methods, one must solve a set of coupled equations for the deterministic coefficients of the PCE. This increases the computational effort when the number of coefficients is large. In the original form of PCE, it is based on the Hermite polynomial expansions in terms of Gaussian random variables. Xiu et al. generalized the formulation into Wiener-Askey polynomial basis for other types of random variables, which they called generalized polynomial chaos expansion (gPC) [31–33].

To overcome the difficulty for solving the coupled system, the stochastic collocation method (SCM) was first proposed by Tatang et al. [26]. It is successfully applied and made more practical in [18, 29, 30, 34]. In this approach, the random variables are represented by Lagrange interpolation polynomials and one can derive an uncoupled system

for the expansion coefficients at selected positions. The solution process is highly parallelizable and it is quite promising. For the current construction of SCM, the selected points for the expansion coefficients are either tensor products of one dimensional Gaussian quadrature points, which is computationally too expensive; or Stroud 2 or 3 quadrature points, which is computationally inexpensive but not accurate enough; or Smolyak sparse grids which is accurate enough and computationally acceptable but it is still desirable to find more easily implementable methods. In this paper, we propose an efficient and accurate candidate, to which we refer as *adaptive Stroud SCM*.

We combined the Karhunen-Loève expansion (KLE) with the Stroud SCM to present a new method — the adaptive Stroud SCM — for uncertainty analysis of flow in random porous media in this paper. Through the analysis for the one-dimensional problem, we observe that the solution is smoother for high modes in probability space. A rough error analysis of Stroud SCM suggests that the main error comes from the first-order derivative with respect to the low modes in probability space. This motivates us to subdivide the leading dimensions in KLE, and we apply Stroud SCM in these subdivided elements. It can be viewed as a kind of mixture of the h -version FEM and the collocation method. This approach is appealing because it results in independent deterministic differential equations, which can be easily implemented with existing codes, and it is accurate enough. We applied the adaptive Stroud SCM to several cases of one- and two-dimensional flows in random porous media, with different spatial variabilities and correlation lengths. The comparisons with the MC, the tensor products SCM and the quasi-MC SCM are also performed. The numerical results show the efficiency and accuracy of our proposed method. Similar adaptive idea for SPDEs is also proposed in [27, 28] independently.

The rest of the paper is organized as follows. In Section 2, we first review the governing equations for random porous medium flow and the basics of the standard framework for SCM. In Section 3, we review the KLE applied to the SPDE and how to transform it into the standard SCM framework. Then we present our adaptive Stroud SCM in Section 4. In Section 5, we apply our method to one- and two-dimensional porous medium flow and make comparisons to other methods. Finally we draw some conclusions.

2 Governing equations and standard SCM

2.1 Stochastic differential equations

The steady-state flow in saturated porous media with uncertainty satisfies the continuity equation and Darcy's law:

$$\nabla \cdot \mathbf{q}(\omega, \mathbf{x}) = g(\omega, \mathbf{x}), \quad \omega \in \Omega, \mathbf{x} \in D, \quad (2.1)$$

$$\mathbf{q}(\omega, \mathbf{x}) = -K_s(\omega, \mathbf{x}) \nabla h(\omega, \mathbf{x}), \quad (2.2)$$

subject to boundary conditions

$$h(\omega, \mathbf{x}) = H(\omega, \mathbf{x}), \quad \mathbf{x} \in \Gamma_D, \quad (2.3)$$

$$\mathbf{q}(\omega, \mathbf{x}) \cdot \mathbf{n}(\mathbf{x}) = Q(\omega, \mathbf{x}), \quad \mathbf{x} \in \Gamma_N, \quad (2.4)$$

where $\mathbf{q}(\omega, \mathbf{x})$ is the specific discharge (flux), $g(\omega, \mathbf{x})$ is the source (or sink) term, $K_s(\omega, \mathbf{x})$ is the hydraulic conductivity, and $h(\omega, \mathbf{x})$ is hydraulic head. $H(\omega, \mathbf{x})$ is the prescribed head on Dirichlet boundary segments Γ_D , and $Q(\omega, \mathbf{x})$ is the prescribed flux across Neumann boundary segments Γ_N . Here $\mathbf{n}(\mathbf{x}) = (n_1, \dots, n_d)^T$ is the unit outer normal vector on the boundary $\Gamma = \Gamma_D \cup \Gamma_N$. All of the functions depending on $\omega \in \Omega$ means that they are random variables. In this case, the above system forms stochastic partial differential equations (SPDE), which possess many challenging computational problems [37]. For simplicity, we will in this paper only consider the uncertainty coming from K_s .

2.2 Review of standard SCM formulation

Suppose a SPDE only depends on random variables $\boldsymbol{\xi} = (\xi_1, \xi_2, \dots, \xi_N)^T$ which take values in the space P after suitable discretization of the probability space Ω . In an abstract form we denote it as

$$\mathcal{L}(u; \boldsymbol{\xi}, \mathbf{x}) = f(\boldsymbol{\xi}, \mathbf{x}), \quad \boldsymbol{\xi} \in P, \mathbf{x} \in D, \quad (2.5)$$

where \mathcal{L} is an operator acting on u and depending on the spatial coordinates \mathbf{x} and the random vector $\boldsymbol{\xi}$, and f is a known function. Here we omit the boundary conditions for simplicity. Suppose $\boldsymbol{\xi}$ has probability density $\rho(\boldsymbol{\theta})$, where θ_i is the dummy variable corresponding to ξ_i ($1 \leq i \leq N$). In the numerical solution, Eq. (2.5) is usually represented in a weak form: To seek $u(\boldsymbol{\theta}, \mathbf{x}) \in V$ such that

$$\int_P \rho(\boldsymbol{\theta}) \mathcal{L}(u; \boldsymbol{\theta}, \mathbf{x}) v(\boldsymbol{\theta}) d\boldsymbol{\theta} = \int_P \rho(\boldsymbol{\theta}) f(\boldsymbol{\theta}, \mathbf{x}) v(\boldsymbol{\theta}) d\boldsymbol{\theta}, \quad \forall v(\boldsymbol{\theta}) \in W, \quad (2.6)$$

where V is called the trial function space, and W is called the test function space. The specification of V and W forms different choices of stochastic finite element or collocation methods for SPDE in probability space [12,15]. The obtained system depends on \mathbf{x} , which can be further discretized in the space D to get the final numerical solution.

The construction of standard SCM is based on polynomial approximation in the space P . For simplicity of exposition we suppose $P = [-1, 1]^N$ and $\boldsymbol{\Theta} = \{\boldsymbol{\theta}_i\}_{i=0}^M \subset P$ be a set of prescribed interpolation nodes. Denote by $\{L_i(\boldsymbol{\theta})\}_{i=0}^M$ the corresponding Lagrange interpolation basis functions. For any function $u(\boldsymbol{\theta}) \in C(P)$, define the polynomial interpolation $\mathcal{I}(u)$ as

$$\mathcal{I}(u)(\boldsymbol{\theta}) = \sum_{i=0}^M u(\boldsymbol{\theta}_i) L_i(\boldsymbol{\theta}). \quad (2.7)$$

Now we define

$$V = \text{span}\{L_i(\boldsymbol{\theta})\}_{i=0}^M, \quad W = \text{span}\{\delta(\boldsymbol{\theta} - \boldsymbol{\theta}_i)\}_{i=0}^M, \quad (2.8)$$

we obtain the SCM discretization of Eq. (2.6),

$$\mathcal{L}(u_i(\mathbf{x}); \boldsymbol{\theta}_i, \mathbf{x}) = f(\boldsymbol{\theta}_i, \mathbf{x}), \quad (2.9)$$

where $u_i(\mathbf{x}) = u(\boldsymbol{\theta}_i, \mathbf{x})$. Note that *this system is decoupled and formally does not depend on the choice of the basis functions*. Furthermore, we can approximate the mean and variance of the function u through (2.7),

$$\langle u(\boldsymbol{\xi}) \rangle = \int_P u(\boldsymbol{\theta}) \rho(\boldsymbol{\theta}) d\boldsymbol{\theta} \simeq \sum_{i=0}^M u(\boldsymbol{\theta}_i) \int_P L_i(\boldsymbol{\theta}) \rho(\boldsymbol{\theta}) d\boldsymbol{\theta} = \sum_{i=0}^M u_i w_i, \quad (2.10)$$

$$\begin{aligned} \text{Var}(u(\boldsymbol{\xi})) &= \int_P u^2(\boldsymbol{\theta}) \rho(\boldsymbol{\theta}) d\boldsymbol{\theta} - \left(\int_P u(\boldsymbol{\theta}) \rho(\boldsymbol{\theta}) d\boldsymbol{\theta} \right)^2 \\ &\simeq \sum_{i=0}^M u^2(\boldsymbol{\theta}_i) \int_P L_i(\boldsymbol{\theta}) \rho(\boldsymbol{\theta}) d\boldsymbol{\theta} - \left(\sum_{i=0}^M u(\boldsymbol{\theta}_i) \int_P L_i(\boldsymbol{\theta}) \rho(\boldsymbol{\theta}) d\boldsymbol{\theta} \right)^2 \\ &= \sum_{i=0}^M u_i^2 w_i - \left(\sum_{i=0}^M u_i w_i \right)^2, \end{aligned} \quad (2.11)$$

where $\{w_i\}_{i=0}^M$ are the corresponding quadrature weights.

In summary, the numerical solution of a SPDE is transformed into a high-dimensional quadrature problem with SCM. And the construction of a concrete SCM is composed of two sets of parameters: the interpolation nodes and the quadrature weights. In the next subsections, we will discuss some existing choices and develop a new method in Section 4.

2.2.1 Tensor product of one-dimensional nodal sets

The tensor product of one-dimensional quadrature points is a natural choice of the nodal set. When $N = 1$, there are many good interpolation formulas for smooth functions $u : [-1, 1] \rightarrow \mathbb{R}$, i.e., for each direction $i = 1, \dots, N$, we can construct a one-dimensional interpolation

$$\mathcal{I}_i(u) = \sum_{k=1}^{m_i} u(\theta_i^k) \cdot a_i^k \quad (2.12)$$

based on nodal sets

$$\boldsymbol{\Theta}_i = (\theta_i^1, \dots, \theta_i^{m_i}) \subset [-1, 1], \quad (2.13)$$

where $a_i^k = a^k(\theta_i)$ is the 1D interpolation basis polynomial at θ_i^k . The quadrature weights can be easily found from standard numerical analysis book [22]. For the multivariate case, the nodal set is taken as the tensor product $\boldsymbol{\Theta}_1 \otimes \dots \otimes \boldsymbol{\Theta}_N$, and the interpolation polynomial

$$\mathcal{I}(u) \equiv (\mathcal{I}_1 \otimes \dots \otimes \mathcal{I}_N)(u) = \sum_{k_1=1}^{m_1} \dots \sum_{k_N=1}^{m_N} u(\theta_1^{k_1}, \dots, \theta_N^{k_N}) \cdot (a_1^{k_1} \otimes \dots \otimes a_N^{k_N}). \quad (2.14)$$

It is easy to extend the Lagrange formulas to this case, as can be found in [3, 14]. However, if we use the same interpolating function (2.12) for each dimension with the same number of points, i.e., $m_1 = \dots = m_N \equiv m$, the total number of points is $M = m^N$. This number grows quickly in high dimensions with $N \gg 1$. This property makes the tensor product nodal set difficult to be implemented practically.

2.2.2 Quasi-Monte Carlo method

Another natural choice of the nodal set for high-dimensional integration in a cube is quasi-Monte Carlo method (QMC) [21, 22]. After generating deterministic quasi-random numbers, for example the Sobol, Halton or Faure sequence, QMC approximates the integration through a sample average with equal weight for each node. Mathematically, suppose $\Theta = \{\theta_i\}_{i=0}^M \subset [0, 1]^N$ be a prescribed quasi-random sequence, we can approximate the integration of the function u as

$$\int_{[0,1]^N} u(\theta) d\theta \simeq \frac{1}{M+1} \sum_{i=0}^M u(\theta_i). \quad (2.15)$$

For the Gaussian random variables or the random variables taking values in $[-1, 1]^N$, we can make a straightforward change of variable to the case considered above. This will be discussed later in detail.

2.2.3 Stroud-2 cubature method

For $P = [-1, 1]^N$, Stroud constructed a set of cubature points with $(N+1)$ -point that is accurate for multiple integrals of polynomials of degree 2 [25]. The degree 2 formula, termed the Stroud-2 method hereafter, consists of points $\{\theta_i\}_{i=0}^N$ such that

$$\theta_i^{2r-1} = \sqrt{\frac{2}{3}} \cos \frac{2ri\pi}{N+1}, \quad \theta_i^{2r} = \sqrt{\frac{2}{3}} \sin \frac{2ri\pi}{N+1}, \quad r = 1, 2, \dots, [N/2], \quad (2.16)$$

where $[N/2]$ is the greatest integer not exceeding $N/2$, and if N is odd $\theta_i^N = (-1)^i / \sqrt{3}$. The quadrature weight is $w_i = 1/(N+1)$, $i = 0, 1, \dots, N$.

The Stroud-2 method employs the minimal number of points for its corresponding algebraic accuracy [19]. The method is quite simple and easy to implement, but once N is prescribed, there is no way to decrease the error by adding more collocation points, which is a drawback of this method. One basic motivation of our work is to improve the Stroud method with relative simple strategy.

3 KL based SCM for porous media flow

3.1 Karhunen-Loève expansion

Let $Y(\omega, x) = \ln[K_s(\omega, x)]$ be a random field. One may write $Y(\omega, x) = \langle Y(\omega, x) \rangle + Y'(\omega, x)$, where $\langle Y(\omega, x) \rangle$ is the mean and $Y'(\omega, x)$ is the fluctuation. In practice, $Y'(\omega, x)$ is usually

approximated as a Gaussian random field. Its spatial structure may be described by the covariance function $C_Y(\mathbf{x}_1, \mathbf{x}_2) = \langle Y'(\omega, \mathbf{x}_1) Y'(\omega, \mathbf{x}_2) \rangle$. Since the covariance function is bounded, symmetric and positive-definite, it may be decomposed as [7]

$$C_Y(\mathbf{x}_1, \mathbf{x}_2) = \sum_{n=1}^{\infty} \lambda_n f_n(\mathbf{x}_1) f_n(\mathbf{x}_2), \quad (3.1)$$

where λ_n and $f_n(\mathbf{x})$ are called eigenvalues and eigenfunctions, respectively, and $f_n(\mathbf{x})$ are orthogonal and deterministic functions that form a complete set [16],

$$\int_D f_n(\mathbf{x}) f_m(\mathbf{x}) d\mathbf{x} = \delta_{nm}, \quad n, m \geq 1. \quad (3.2)$$

Eigenvalues and eigenfunctions can be solved from the following Fredholm equation:

$$\int_D C_Y(\mathbf{x}_1, \mathbf{x}_2) f(\mathbf{x}_2) d\mathbf{x}_2 = \lambda f(\mathbf{x}_1). \quad (3.3)$$

Then the random process $Y(\omega, \mathbf{x})$ can be expressed as

$$Y(\omega, \mathbf{x}) = \langle Y(\omega, \mathbf{x}) \rangle + \sum_{n=1}^{\infty} \alpha_n \sqrt{\lambda_n} f_n(\mathbf{x}), \quad (3.4)$$

where α_n are independently, and identically distributed (i.i.d.) Gaussian random variables with mean zero and variance one. The expansion in Eq. (3.4) is called the Karhunen-Loève expansion. This expansion, which is a spectral expansion, is optimal in the sense of mean square convergence [12].

Although, in general, the eigenvalue problem (3.3) has to be solved numerically, λ_n and $f_n(\mathbf{x})$ can be found analytically for some special types of covariance functions. If a one-dimensional stochastic process with a covariance function,

$$C_Y(x_1, x_2) = \sigma_Y^2 \exp(-|x_1 - x_2|/\eta), \quad (3.5)$$

where σ_Y^2 and η are the variance and the correlation length of the process, respectively, the eigenvalues and their corresponding eigenfunctions can be expressed as in [12, 38],

$$\lambda_n = \frac{2\eta\sigma_Y^2}{\eta^2\omega_n^2 + 1}, \quad (3.6)$$

and

$$f_n(x) = \frac{1}{\sqrt{(\eta^2\omega_n^2 + 1)L/2 + \eta}} [\eta\omega_n \cos(\omega_n x) + \sin(\omega_n x)], \quad (3.7)$$

where ω_n are positive roots of the characteristic equation

$$(\eta^2\omega^2 - 1) \sin(\omega L) = 2\eta\omega \cos(\omega L). \quad (3.8)$$

So we have the derivative of the eigenfunction with respect to x as

$$f_n'(x) = \frac{1}{\sqrt{(\eta^2 \omega_n^2 + 1)L/2 + \eta}} [-\eta \omega_n^2 \sin(\omega_n x) + \omega_n \cos(\omega_n x)]. \quad (3.9)$$

Eq. (3.8) has an infinite number of positive roots. Sorting these roots ω_n in an increasing order, the related eigenvalues λ_n are monotonically decreasing. The decay rate of λ_n determines the number of terms that are retained in the Karhunen-Loève expansion, which equals the random dimensionality of our problem.

For problems in two dimensions, we suppose that the covariance function is

$$C_Y(\mathbf{x}, \mathbf{y}) = \sigma_Y^2 \exp(-|x_1 - y_1|/\eta_1 - |x_2 - y_2|/\eta_2)$$

for a rectangular domain $D = \{(x_1, x_2) : 0 \leq x_1 \leq L_1, 0 \leq x_2 \leq L_2\}$. Eq. (3.3) can be solved independently for x_1 and x_2 directions to obtain the eigenvalues $\lambda_n^{(1)}$ and $\lambda_n^{(2)}$, and the eigenfunctions $f_n^{(1)}(x_1)$ and $f_n^{(2)}(x_2)$. These eigenvalues and eigenfunctions are then combined to form the eigenvalues and eigenfunctions of C_Y :

$$\lambda_n = \frac{4\eta_1\eta_2\sigma_Y^2}{[\eta_1^2(\omega_i^{(1)})^2 + 1][\eta_2^2(\omega_j^{(2)})^2 + 1]}, \quad (3.10)$$

$$f_n(\mathbf{x}) = f_n(x_1, x_2) = f_i^{(1)}(x_1) f_j^{(2)}(x_2), \quad (3.11)$$

where $\omega_i^{(1)}$ and $\omega_j^{(2)}$ are two series of positive roots of (3.8) using parameters (L_1, η_1) and (L_2, η_2) , respectively. Here we assume that the indices i and j are mapping to the index n in such a way that the λ_n form a nonincreasing series.

3.2 Transforming to SCM framework

Truncating Eq. (3.4) with $N+1$ terms, we reduce the original system into a SPDE only depending on $\alpha_1, \dots, \alpha_N$. Denote the cumulative distribution function (CDF) of α_i by $\mathcal{F}(\alpha)$ and suppose that

$$F(\alpha) = 2\mathcal{F}(\alpha) - 1. \quad (3.12)$$

It is straightforward to see $\xi_i = F(\alpha_i)$ is uniformly distributed in $[-1, 1]$. Then $Y(\omega, \mathbf{x})$ can be approximated as

$$Y(\xi, \mathbf{x}) = \langle Y(\omega, \mathbf{x}) \rangle + \sum_{i=1}^N F^{-1}(\xi_i) \sqrt{\lambda_i} f_i(\mathbf{x}). \quad (3.13)$$

This transforms to the standard setup for SCM. With chosen quadrature nodes $\{\theta_i\}_{i=0}^M$, we have the following SCM form,

$$\nabla \cdot \mathbf{q}(\theta_i, \mathbf{x}) = g(\mathbf{x}), \quad \mathbf{x} \in D, \quad (3.14)$$

$$\mathbf{q}(\theta_i, \mathbf{x}) = -\exp(Y(\theta_i, \mathbf{x})) \nabla h(\theta_i, \mathbf{x}), \quad (3.15)$$

subject to the boundary conditions

$$h(\boldsymbol{\theta}_i, \mathbf{x}) = H(\mathbf{x}), \quad \mathbf{x} \in \Gamma_D, \quad (3.16)$$

$$\mathbf{q}(\boldsymbol{\theta}_i, \mathbf{x}) \cdot \mathbf{n}(\mathbf{x}) = Q(\mathbf{x}), \quad \mathbf{x} \in \Gamma_N. \quad (3.17)$$

We will apply the numerical discretization to the 1D and 2D cases for this system in Section 5.

4 Adaptive Stroud SCM

4.1 Exact solution for 1D case

Let us first consider one-dimensional flow and assume the forcing term $g(\mathbf{x})$ to be zero. Hence the governing equation of the flow can be expressed as

$$\frac{d}{dx} \left[\exp(Y(\omega, x)) \frac{d}{dx} h(\omega, x) \right] = 0, \quad (4.1)$$

with the boundary conditions,

$$h(\omega, x) = H_0, \quad x = 0; \quad h(\omega, x) = H_L, \quad x = L, \quad (4.2)$$

where $Y(\omega, x) = \ln K_s(\omega, x)$. It is not difficult to get the analytic solution of Eqs. (4.1) and (4.2),

$$h(\omega, x) = (H_L - H_0) \frac{\int_0^x \exp(-Y(\omega, y)) dy}{\int_0^L \exp(-Y(\omega, y)) dy} + H_0, \quad x \in [0, L]. \quad (4.3)$$

If $Y(\omega, x)$ is approximated with KL expansion (3.13), then we take differentiation with respect to ξ_i to obtain

$$\frac{\partial h(\boldsymbol{\xi}, x)}{\partial \xi_i} = -\sqrt{\lambda_i} (H_L - H_0) \frac{dF^{-1}(\xi_i)}{d\xi_i} \cdot \frac{(G_i(\boldsymbol{\xi}, x)H(\boldsymbol{\xi}, L) - G_i(\boldsymbol{\xi}, L)H(\boldsymbol{\xi}, x))}{(H(\boldsymbol{\xi}, L))^2}, \quad (4.4)$$

where

$$G_i(\boldsymbol{\xi}, x) = \int_0^x \exp(-Y(\boldsymbol{\xi}, y)) f_i(y) dy, \quad (4.5)$$

$$H(\boldsymbol{\xi}, x) = \int_0^x \exp(-Y(\boldsymbol{\xi}, y)) dy. \quad (4.6)$$

On the other hand, from Eq. (3.8) one can find the solutions $\omega_n \sim n\pi/L$ for large n , which means that λ_n defined by (3.6) decreases at a rate of $1/n^2$. The definition of eigenfunctions, (3.7), shows $|f_n(x)|$ are bounded. So formally we get the smoothness information of h in the space for random variables

$$\left| \frac{\partial h(\boldsymbol{\xi}, x)}{\partial \xi_i} \right| \sim \mathcal{O}\left(\frac{1}{i}\right), \quad i = 1, 2, \dots, N, \quad (4.7)$$

after ignoring some common factors for different i . One can see from (4.7) that $h(\boldsymbol{\zeta}, x)$ is smoother in the ζ_i -direction when i is large. Similar estimates can also be obtained for second-order derivatives to $\boldsymbol{\zeta}$,

$$\left| \frac{\partial^2 h(\boldsymbol{\zeta}, x)}{\partial \zeta_i \partial \zeta_j} \right| \sim \mathcal{O}\left(\frac{1}{ij}\right), \quad i, j = 1, 2, \dots, N. \quad (4.8)$$

This information is our basic motivation for a modified Stroud method. A more rigorous analysis on the eigenvalue decay of KL expansion can be found in [24].

4.2 Adaptive Stroud collocation method

A rough analysis [11] shows that the Stroud cubature error depends on the first and second derivatives of the integrand. The analysis in the last subsection suggests that the leading error terms come from the first derivative with respect to ζ_i when i is small. This heuristic estimate is quite instructive for constructing new methods. Recalling the drawback of the direct Stroud method is that there is no way to decrease the error by adding more collocation points if the dimension N is prescribed, we propose to improve the Stroud method as follows. To get a more accurate result, we need to subdivide the space $[-1, 1]^N$ into some small parts and take the integral in each part. But the crux of the matter is to *just subdivide the leading dimensions of h in the $\boldsymbol{\theta}$ space since the variation in the remaining dimensions is relatively smooth on the basis of the analysis (4.7)*. This technique is only applicable to cases where the spatial structure of the underlying random fields (like the hydraulic conductivity in our example) is known *a priori*, such as with the KL-type expansion. We call this modified algorithm — adaptive Stroud collocation method.

Mathematically, let $\{P_j\}_{j=1}^K$ express the partitions of P . By affine transformation, using the collocation points of the Stroud-2 method, one can get the points in P_j , $\{\boldsymbol{\theta}_i^j\}_{i=0}^N$. So the approximations about the mean and variance of $h(\boldsymbol{\zeta})$ are

$$\langle h(\boldsymbol{\zeta}) \rangle = \int_{[0,1]^N} h(\boldsymbol{\theta}) \rho(\boldsymbol{\theta}) d\boldsymbol{\theta} \simeq \frac{2^N}{K(N+1)} \sum_{i=0}^N \sum_{j=1}^K h(\boldsymbol{\theta}_i^j) \rho(\boldsymbol{\theta}_i^j), \quad (4.9)$$

$$\begin{aligned} & \text{Var}(h(\boldsymbol{\zeta})) \\ &= \int_{[0,1]^N} h^2(\boldsymbol{\theta}) \rho(\boldsymbol{\theta}) d\boldsymbol{\theta} - \left(\int_{[0,1]^N} h(\boldsymbol{\theta}) \rho(\boldsymbol{\theta}) d\boldsymbol{\theta} \right)^2 \\ &\simeq \frac{2^N}{K(N+1)} \sum_{i=0}^N \sum_{j=1}^K h^2(\boldsymbol{\theta}_i^j) \rho(\boldsymbol{\theta}_i^j) - \left(\frac{2^N}{K(N+1)} \sum_{i=0}^N \sum_{j=1}^K h(\boldsymbol{\theta}_i^j) \rho(\boldsymbol{\theta}_i^j) \right)^2. \end{aligned} \quad (4.10)$$

We will apply this method to the steady-state porous media flow in Section 5. The results will be presented in detail there.

4.3 Summary

From the previous analysis we conclude:

1. The Stroud-2 SCM presents the best choice of collocation points to get the degree of exactness 2. However, there is no way to improve the accuracy for the standard Stroud method. In order to get a better result, we propose the adaptive Stroud collocation method to divide the leading dimensions of h in the θ space.
2. Assume M' , the number of dimensions, to be divided and I the partition number for each dimension, we often take I and M' small in practice, which does not increase the computational effort very much. And it is enough to decrease the error in evidence, as is shown in Section 5. For the concrete choice of I and M' , we get them by the energy ratios. The details will be shown in Section 5.

5 Results and discussions

5.1 Illustrative examples in 1D

In this and the following subsections we present numerical examples to illustrate the KL based adaptive Stroud SCM and examine its validity and applicability to flow in porous media.

At first, we consider a one-dimensional domain of length $L = 10.0[L]$ (where $[L]$ denotes any consistent length unit). The boundary conditions are prescribed heads at the two ends, $H_0 = 7.0[L]$ and $H_L = 5.0[L]$. The mean of the log hydraulic conductivity is given as $\langle Y \rangle = 0.0$. In the first example, the variance is $\sigma_Y^2 = 1.0$ and the correlation length $\eta = 4.0$.

The eigenvalues and eigenfunctions, λ_n and $f_n(x)$ ($n = 1, 2, \dots$), can be determined analytically by solving Eqs. (3.6) and (3.7). The eigenvalues are monotonically decreasing as illustrated in Fig. 1(a) for cases with different correlation lengths ($\eta = 2$ and 4). Fig. 1(b) shows the sum of eigenvalues as a function of the number of included terms. From Eq. (3.1) we have

$$\sigma_Y^2 = \sum_{n=1}^{\infty} \lambda_n f_n^2(x).$$

Since $\{f_n(x)\}$ forms a complete basis, we have

$$meas(D)\sigma_Y^2 = \sum_{n=1}^{\infty} \lambda_n$$

by integration, where $meas(D)$ is the measure of the domain size (length, area, or volume for 1D, 2D, or 3D domains, respectively). On the other hand, λ_n expresses the energy and input information of random for each term. Usually, to assure that enough random information is included, we suppose the ratio of input energy to total energy, $\sum_{n=1}^N \lambda_n / (meas(D)\sigma_Y^2)$, is larger than a constant β_1 . Owing to the rapid decay, we take

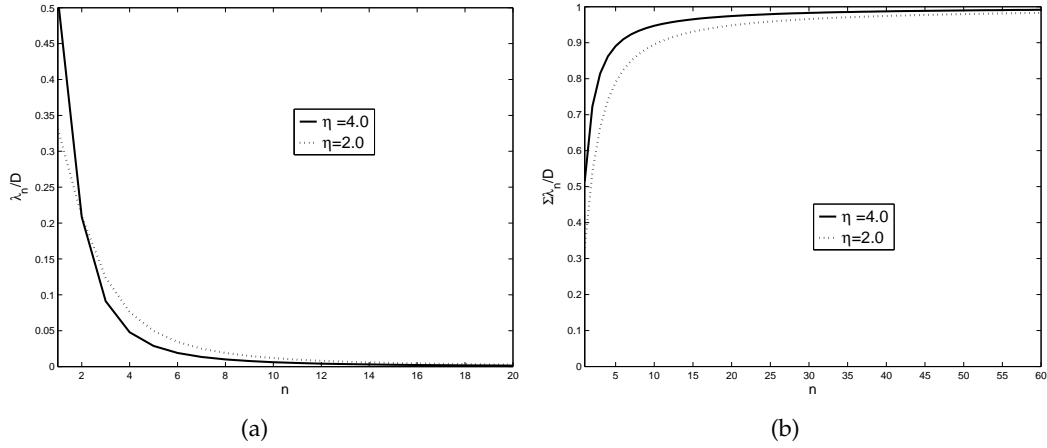


Figure 1: Series of eigenvalues (a) and their finite sums (b), for $\eta = 4.0$ and $\eta = 2.0$, $\sigma_Y^2 = 1.0$.

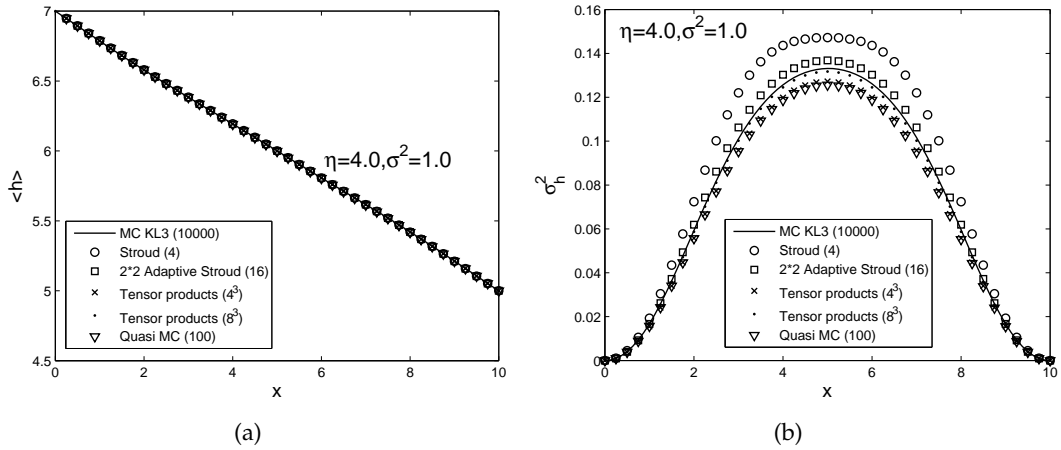


Figure 2: Comparisons of the mean and variance of hydraulic head derived from MC, and SCMs, for $\eta = 4.0$ and $\sigma_Y^2 = 1.0$.

$\beta_1 = 0.8$ in the computation, which means only the first 3 terms are retained in the KL expansion for $\eta = 4.0$. So we have a three-dimensional space for the random variables ζ .

In the computations, we apply the finite difference method to solve Eq. (4.1) and 41 physical nodes are chosen for all SCMs. For the adaptive Stroud SCM, in order to ensure the subdivided leading dimensions cover enough input random information, we suppose the energy ratio of $\sum_{n=1}^{M'} \lambda_n / \sum_{n=1}^N \lambda_n$ is larger than a constant β_2 . Like β_1 , we take $\beta_2 = 0.8$ in the computation. This means only the first 2 dimensions are needed to be subdivided when $\eta = 4.0$ and we choose to halve these dimensions.

Figs. 2(a) and 2(b) show the mean and variance of hydraulic head, respectively, obtained from SCM with Stroud, adaptive Stroud, tensor products of 4 Gauss points, tensor products of 8 Gauss points, QMC as well as the direct sampling Monte Carlo method.

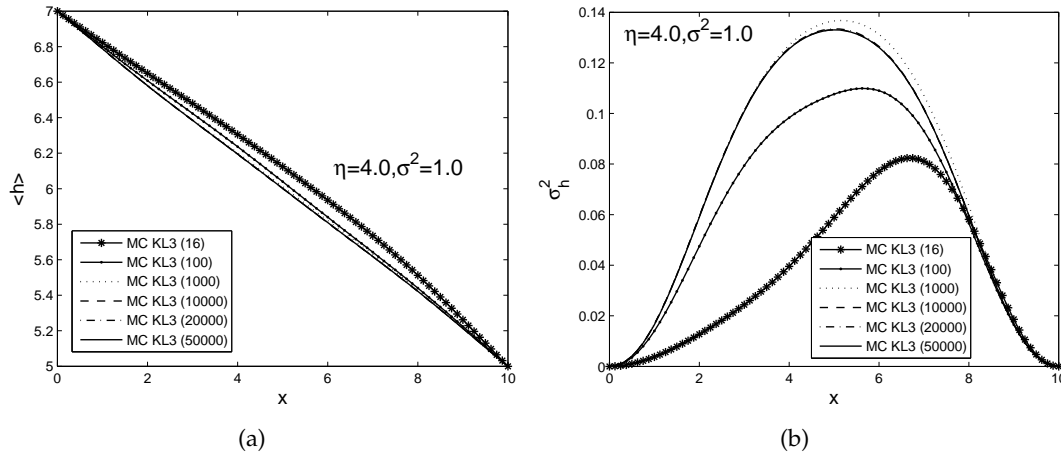


Figure 3: The mean and variance of hydraulic head derived from 4 sets of Monte Carlo simulations, corresponding to 16, 100, 1000, and 10,000 realizations, for $\eta = 4.0$ and $\sigma_Y^2 = 1.0$.

There is a solution of the '2*2' adaptive Stroud SCM, where '2' means the first two dimensions of the random variable ξ are subdivided, and 2' means each dimension is divided into 2 parts. Correspondingly, '2*3' means that each dimension is divided into 3 parts for the first 2 dimensions of ξ , etc.

Since only 3 terms are retained in the KL expansion in this case, the Stroud SCM needs 4 collocation points. For the '2*2' adaptive Stroud SCM, the number of collocation points needed is 16. The SCMs with tensor products and QMC use 64 and 100 collocation points, respectively. To obtain an accurate solution for comparison, we solve the same problem with the direct sampling Monte Carlo method. We truncate the KL expansion to 3 terms as before to generate the random field of the log hydraulic conductivity based on Eq. (3.4) and make 10,000 realizations in the Monte Carlo simulation to ensure statistical convergence and thus accurate results, which are used as the benchmarks in our study.

Comparisons on computational efforts and the accuracy are made among SCMs and Monte Carlo method. Since the computational efforts for solving Eq. (4.1) for each collocation point in SCMs is the same, the computational complexity is decided by the number of collocation points, i.e., the number of simulations.

Fig. 3 illustrates 6 sets of Monte Carlo simulations, corresponding to 16, 100, 1000, 10000, 20000 and 50000 realizations. It can be found that Monte Carlo simulations with 16 or 100 realizations can not obtain statistically accurate results and that even 1000 realizations are not enough compared to the Monte Carlo results with 10,000 realizations. More realizations improve little which is indistinguishable with eyes. We will take 10,000 realizations for the latter computations. As we have mentioned, only 16 collocation points simulations are needed in the '2*2' adaptive Stroud SCM, it is much less than the number of realizations needed in Monte Carlo method. Obviously, the adaptive Stroud SCM is far more efficient than Monte Carlo method. Both the Monte Carlo method and the adaptive Stroud SCM involve sampling. The difference is that in the Monte Carlo method

realizations are generated randomly, whereas in the adaptive Stroud SCM a structural expression (the polynomial interpolation) of the output random field is generated at first and then the collocation points are adopted according to the adaptive Stroud method.

As we know, the Gauss-Legendre formula has the best algebraic accuracy in 1D. From Section 2.2.1, even we only use 4 Gauss cubature points in every random dimensions, 64 collocation points are needed in the tensor product SCM for this case. It is more than the double of the computational effort for the '2*2' adaptive Stroud SCM. However, from Fig. 2(b), the result of the adaptive Stroud SCM is better. The tensor product with 8 Gauss points in each direction gives highly accurate solution, which matches the MC solution quite well. But the computational effort is too large compared with our adaptive Stroud method. From Fig. 2(b), the adaptive Stroud's result is also better than that of QMC. So the adaptive Stroud SCM efficiently decreases the error of Stroud-type method and it needs the least number of collocation points.

Owing to the particular boundary conditions in our examples, the mean head obtained from different approaches are very close to each other. We thus focus our discussion only on the head variance in the following subsections.

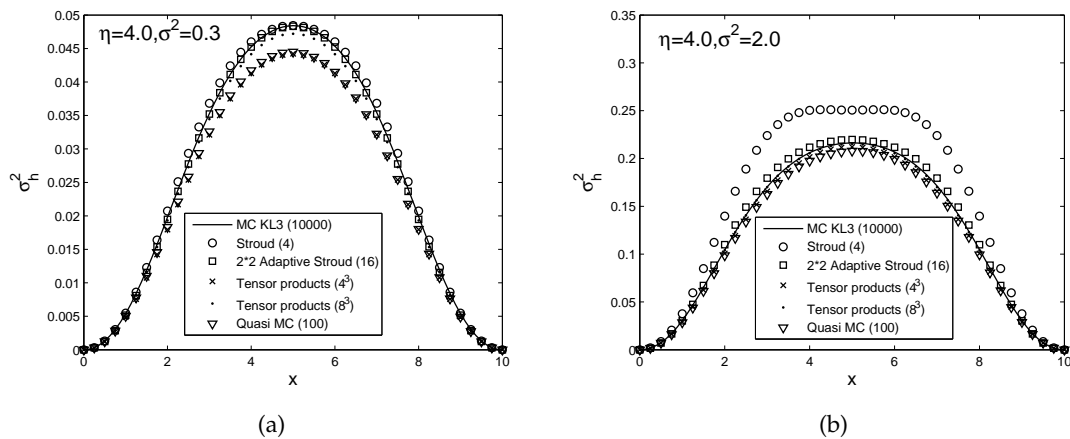


Figure 4: Comparisons of head variance derived from SCMs and MC, with different spatial variability, for $\eta = 4.0$.

To further test the validity of the adaptive Stroud SCM, we have examined two more examples with different spatial variability, while keeping other conditions the same as in the first case. In Fig. 4, we present the comparisons of the head variance derived from the SCMs and Monte Carlo method for $\sigma_Y^2 = 0.3$ and 2. For small spatial variability, i.e., $\sigma_Y^2 = 0.3$, the result from the adaptive Stroud SCM is almost identical to the Monte Carlo result. As the spatial variability becomes large, i.e., $\sigma_Y^2 = 2.0$, the adaptive Stroud SCM agrees with the Monte Carlo result fairly well. This observation is encouraging as the variance of $\sigma_Y^2 = 2.0$, being equivalent to the coefficient of variation of hydraulic conductivity $CV_{K_s} = \sigma_{K_s} / \langle K_s \rangle = 253\%$, represents a large variability in hydraulic conductivity. We will discuss the case of huge spatial variability in Section 5.2.

5.2 Discussions

5.2.1 Effect of correlation length

As shown in Fig. 1, the correlation length η relative to the domain length L controls the rate of decay in the eigenvalues. To further test the effect of correlation length on the SCM approaches, three cases for $\eta=2.0$ with different spatial variabilities $\sigma_Y^2=0.3, 1.0$ and 2.0 , are performed. We also include the Monte Carlo simulation result for comparison. The head variance obtained from those approaches are presented in Fig. 5. Note that the number of physical nodes is also chosen as 41 in SCMs and the number of realizations in Monte Carlo simulations is 10,000. A smaller number of physical nodes or realizations in Monte Carlo simulations could lead to inaccurate results. To ensure the ratio of energy, $\sum_{n=1}^N \lambda_n / (meas(D)\sigma_Y^2)$, is larger than $\beta_1=0.8$, the retained dimension number in the KL expansion for SCMs is chosen as $N=6$. To ensure the ratio of energy, $\sum_{n=1}^{M'} \lambda_n / \sum_{n=1}^N \lambda_n$, is larger than $\beta_2=0.8$, the divided dimension number in adaptive Stroud SCM is chosen as $M'=3$. In this case, we apply tensor product of 2 Gauss points and 8 Gauss points in each direction to make comparison. For the 2^6 integration points, the computational effort is comparable to our adaptive Stroud method (56 points), but the accuracy is worse; for the 8^6 integration points, it is very accurate but the computational effort is too large! From Fig. 5, we observe that for small or moderate spatial variability, i.e., $\sigma_Y^2=0.3$ or 1.0 , the results obtained from the adaptive Stroud SCM agree well with those from Monte Carlo method. When σ_Y^2 is large, i.e., $\sigma_Y^2=2.0$, the adaptive Stroud SCM's result is still close to the Monte Carlo result while the other SCM approaches do not perform well.

5.2.2 Effect of large spatial variability σ_Y^2

As illustrated in the previous sections, for moderate spatial variability, the adaptive Stroud SCM can obtain quite accurate results. In this section, we examine a case with a huge spatial variability, i.e., $\sigma_Y^2=4.0$, corresponding to the coefficient of variation of hydraulic conductivity $CV_{K_s}=732\%$ [37]. If we take $\beta_1=\beta_2=0.8$ for $\eta=4.0$, Fig. 5(d) shows there are some deviations between the adaptive Stroud SCM's result and the MC's in this huge spatial variability case. To improve this result, we increase the energy ratio, $\beta_1=\beta_2=0.9$. The retained dimension number in the KL expansion for SCMs is chosen as $N=6$ and the divided dimension number in adaptive Stroud SCM is chosen as $M'=3$. Meanwhile, the number of collocation points needed in adaptive Stroud SCM is 56 now. It is clear that the more collocation points can efficiently decrease the error and lead to a better result.

5.2.3 Effect of different subdivided dimensions

As we know, adding the collocation points generally can decrease the SCM's error. Since the random vector $\xi = (\xi_1, \xi_2, \dots, \xi_N)^T$, which is used in Section 3, satisfies a uniform distribution. Why do we just divide the leading dimensions, not other dimensions? The reason is the coefficients of $F^{-1}(\xi_i)$ are different in KL expansion (3.13). Since λ_i are

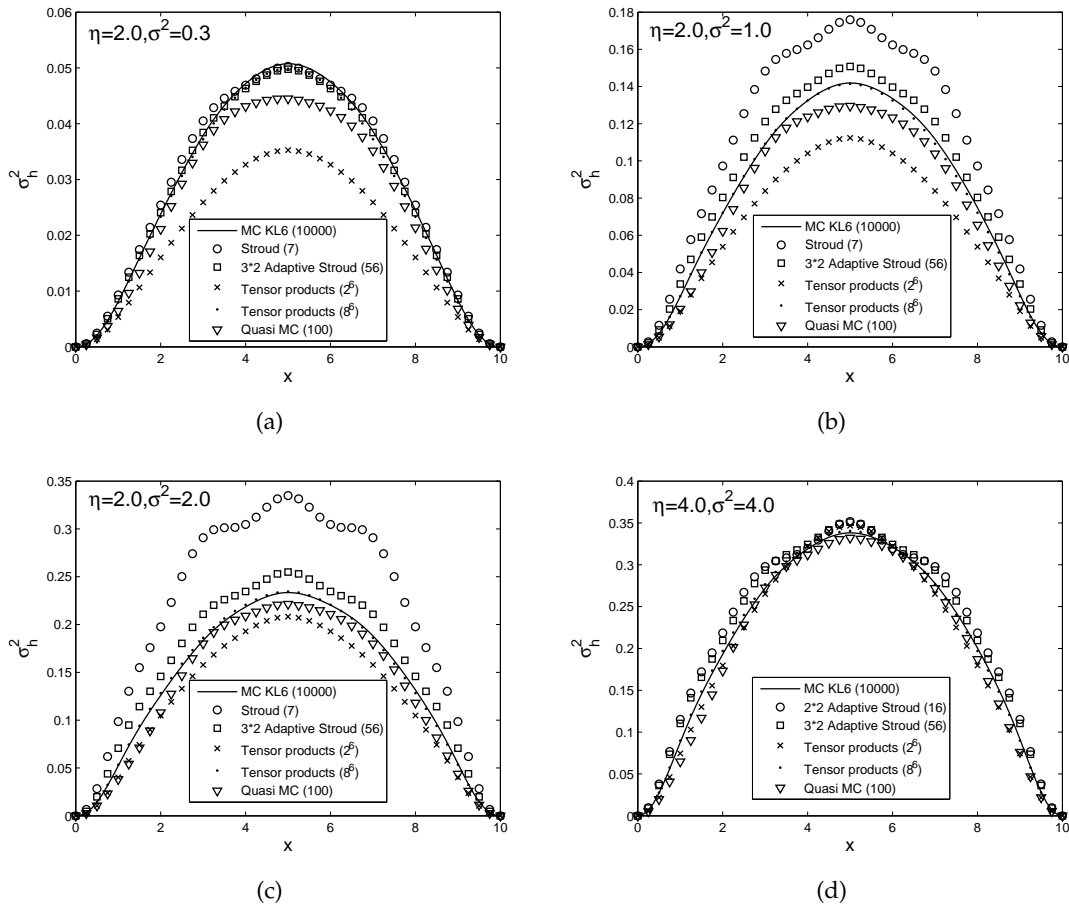


Figure 5: Comparisons of head variance derived from SCMs and MC, with different spatial variability and different correlation length.

monotonically rapidly decreasing, $Y(\xi, x)$ is more sensitive to the leading random dimensions and the variation in the rest dimensions is relatively smooth. Fig. 6 compares the head variance derived from different subdivided dimensions, respectively, for $\eta=4.0$ and $\eta=2.0, \sigma_Y^2=1.0$. In Fig. 6, '0+2*2' expresses to halve the first two dimensions and '2+2*2' expresses to halve the third and fourth dimensions, and so on. The results support our assertion that refining the leading dimensions is effective and sufficient.

5.3 Illustrative examples in 2D

We consider two examples in the two-dimensional case in this section. In the first example, the flow domain is a square of a size $L_1=L_2=10.0[L]$, uniformly discretized into 40×40 square elements. The non-flow conditions are prescribed at the two lateral boundaries. The hydraulic head is prescribed at the left and right boundaries as H_0 and H_L ,

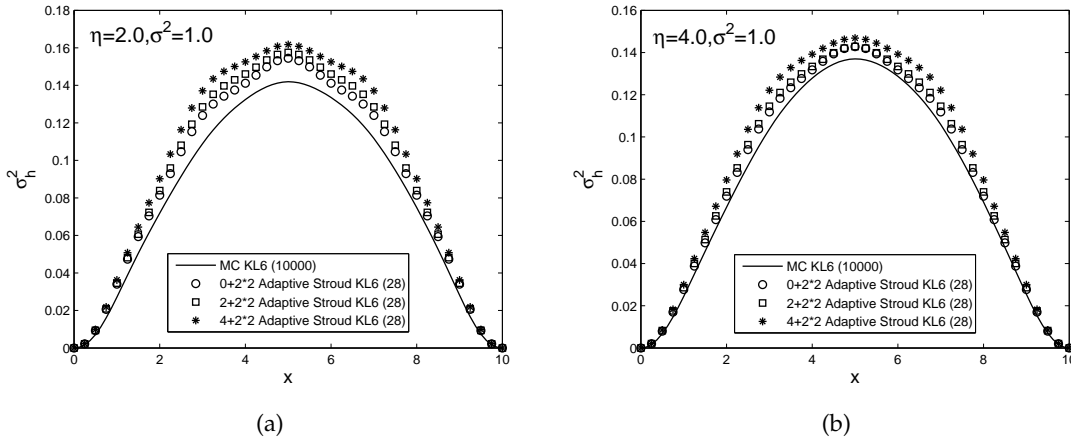


Figure 6: Comparisons of head variance derived from different divided dimensions, for $\eta = 4$ and $\eta = 2$, $\sigma_Y^2 = 1.0$.

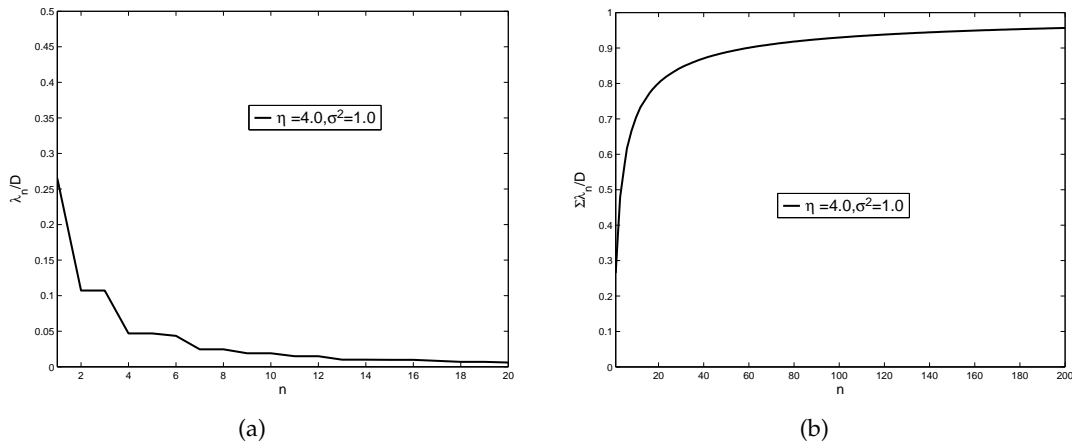


Figure 7: Series of eigenvalues and their finite sums for two-dimensional square flow domain with a separable covariance function, for $\eta = 4.0$ and $\sigma_Y^2 = 1.0$.

respectively, which produces a mean flow from the left to the right. Assume the source (or sink) term, $g(x)$, to be zero. The mean of the log hydraulic conductivity is also given as $\langle Y \rangle = 0.0$. For simplicity, it is assumed in the following examples that the log saturated hydraulic conductivity $Y(\omega, x) = \ln K_s(\omega, x)$ is second-order stationary with a separable exponential covariance function

$$C_Y(x, y) = C_Y(x_1, x_2, y_1, y_2) = \sigma_Y^2 \exp \left[-\frac{|x_1 - y_1|}{\eta} - \frac{|x_2 - y_2|}{\eta} \right]. \tag{5.1}$$

From Eqs. (2.1) and (2.2), for this case the governing equation can be expressed as

$$\frac{\partial^2 h(\omega, x)}{\partial x_1^2} + \frac{\partial^2 h(\omega, x)}{\partial x_2^2} + \frac{\partial Y(\omega, x)}{\partial x_1} \frac{\partial h(\omega, x)}{\partial x_1} + \frac{\partial Y(\omega, x)}{\partial x_2} \frac{\partial h(\omega, x)}{\partial x_2} = 0. \tag{5.2}$$

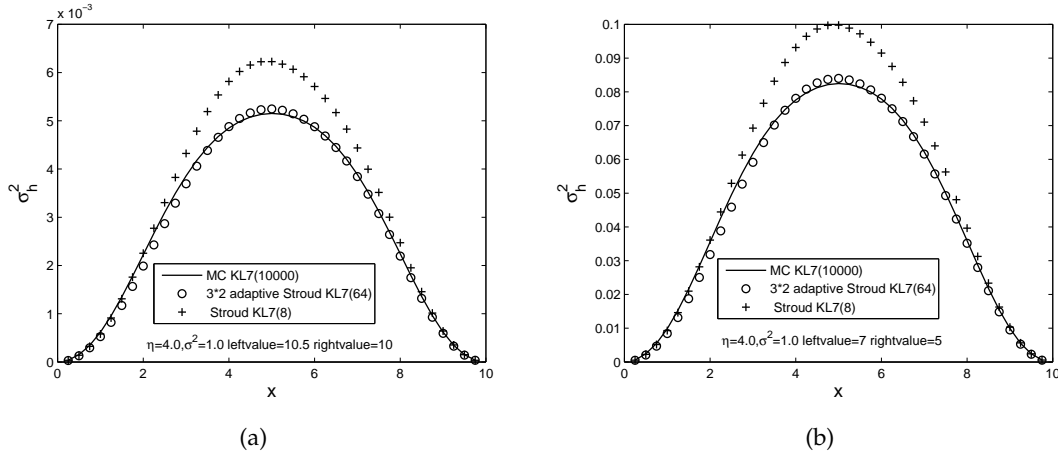


Figure 8: Head variance derived from MC, Stroud SCM and adaptive Stroud SCM at $x_2=5.0$, with different boundary conditions, for $\eta=4.0$ and $\sigma_\gamma^2=1.0$.

Here we suppose $\eta=4.0$ and $\sigma_\gamma^2=1.0$. Fig. 7 shows the series of eigenvalues and their finite sums. By the difference between Fig. 1(a) and Fig. 7(a), one can find the eigenvalue decay ratio in two dimension is slower. To ensure the computational complexity is suitable, we value $\beta_1=0.6$ and $\beta_2=0.8$ in this case. That is, the retained dimension number in the KL expansion for the adaptive Stroud SCM is chosen as $N=7$ and the divided dimension number in the adaptive Stroud SCM is chosen as $M'=3$.

Fig. 8 compares the head variance from the Monte Carlo simulations, the Stroud SCM and the adaptive Stroud SCM along the cross section $x_2=5.0$, for different boundary conditions. In Fig. 8(a), $H_0=10.5[L]$ and $H_L=10.0[L]$. In Fig. 8(b), $H_0=7.0[L]$ and $H_L=5.0[L]$. For comparison, we conduct Monte Carlo simulations using 10,000 two-dimensional realizations generated on the grid of 41×41 nodes with the separable covariance function given in Eq. (5.1), based on Eq. (3.4) with 200 terms. It is shown that the adaptive Stroud SCM can obtain quite accurate results.

In the second case, two wells are located at $(3.0[L], 3.0[L])$ and $(7.0[L], 7.0[L])$ with strengths of $-1.0[L^3/T]$ and $1.0[L^3/T]$ (where T is any consistent time unit). A negative strength represents extraction of fluid out of the domain. We compare results from the Monte Carlo simulations, the Stroud SCM and the adaptive Stroud SCM along the diagonal line which passes both wells, as indicated in Fig. 9.

From Eqs. (2.1) and (2.2), the governing equation can be expressed as

$$\nabla \cdot (K_s(\omega, x) \nabla h(\omega, x)) = -g(x). \quad (5.3)$$

The hydraulic head is prescribed at the left and right boundaries as $H_0=10.5[L]$ and $H_L=10.0[L]$, respectively, while keeping other conditions the same as in the first two-dimensional case. To compare the results in detail, the flow domain is uniformly discretized into 80×80 grids. The steady state, saturated flow equation is solved for each

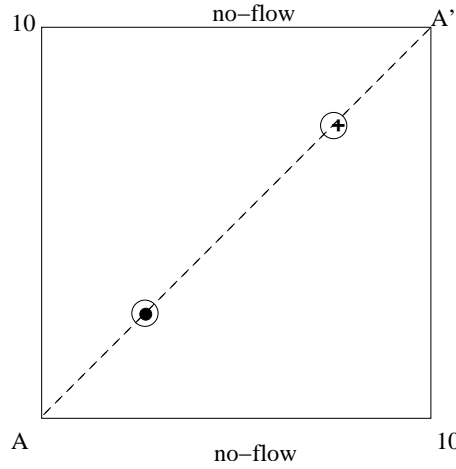


Figure 9: Boundary configuration for the second 2D illustrative example.

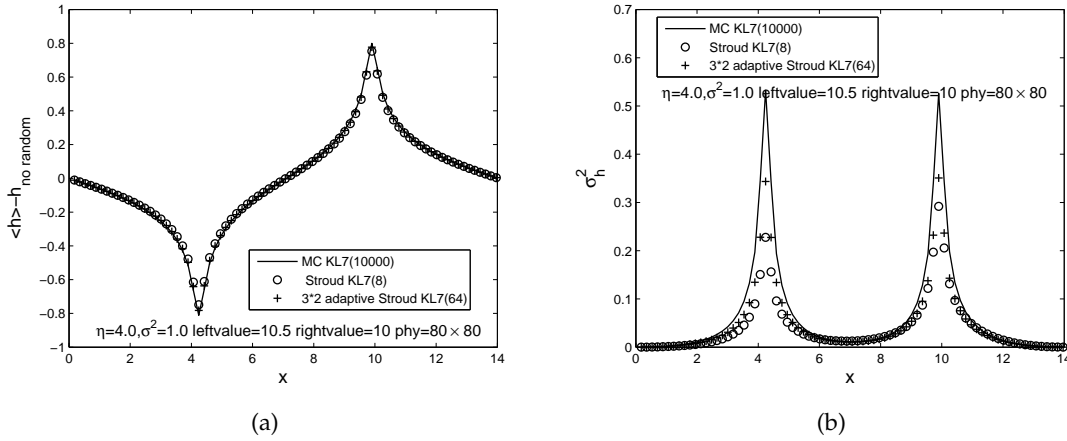


Figure 10: Comparison of (a) detrended mean head and (b) head variance derived from Monte Carlo, Stroud SCM and adaptive Stroud SCM along the diagonal line, for $\eta = 4.0$ and $\sigma_h^2 = 1.0$.

realization of the log hydraulic conductivity, using the finite difference method. The multi-grid method is used to resolve Eq. (5.3). Then, the sample statistics of the flow fields, i.e., the mean predictions of head as well as its associated uncertainty (variance), are computed from realizations.

We compare the results from the Monte Carlo simulations against those from the Stroud SCM and the adaptive Stroud SCM. Due to the particular boundary configuration in our example, the mean head profiles derived from different approaches do not differ significantly. To illustrate their differences more clearly, we plot the detrended mean head rather than the mean head itself. Fig. 10(a) compares the detrended mean head obtained from Monte Carlo simulations, Stroud SCM and adaptive Stroud SCM along the

cross section AA' . It is seen that the mean head from both Stroud and adaptive Stroud SCM are very close to the Monte Carlo results. Fig. 10(b) depicts the comparison of head variance derived from Monte Carlo simulations, Stroud SCM and adaptive Stroud SCM. Although the result of the Stroud SCM shows a pattern similar to that of the Monte Carlo results, the discrepancies are large in well locations. The result of the adaptive Stroud SCM is getting closer to the Monte Carlo result.

6 Conclusions

In this study, we combined the Karhunen-Loève expansion (KLE) with the stochastic collocation method (SCM) to present a new method — the adaptive Stroud SCM — for uncertainty analysis of flow in random porous media. This approach is appealing because it results in independent deterministic differential equations, which similar to the Monte Carlo method, can be implemented with existing codes. We applied the adaptive Stroud SCM to several cases of 1D and 2D flows in random porous media, with different spatial variabilities and correlation lengths. Comparisons with the Monte Carlo method, the tensor products SCM and the QMC SCM are also done. This study leads to the following conclusions:

1. With a relatively small computational effort, the adaptive Stroud method based on KLE is feasible for quantifying uncertainty associated with flow in random porous media, where the random process and stochastic differential equation have to be considered.
2. Similar to the Monte Carlo method, the adaptive Stroud SCM can be easily implemented with existing codes and naturally parallelized.
3. Many covariances of the random log transformed hydraulic conductivity field, $C_Y(x, y)$, can result in the rapid decay of eigenvalues like (3.5), which is taken into account by the adaptive Stroud SCM through subdividing the leading dimensions in probability space. Under certain accuracy, the computational effort of adaptive Stroud SCM is the smallest among the SCMs that we have tried.
4. The energy ratios, β_1 and β_2 , are important to determine the collocation points of the adaptive Stroud SCM. As we have shown, it is enough to have the value of $\beta_1 = \beta_2 = 0.8$ in 1D as a rule. While for larger spatial variability, increasing the value of β_1 and β_2 is needed and the adaptive Stroud SCM remains efficient.

Acknowledgments

T. Li acknowledges the support by National Natural Science Foundation of China (NSFC) grants 10401004, and the National Basic Research Program under the grant 2005CB321704. D. Zhang is grateful to the supports by NSFC through grant 50688901 and by the National Basic Research Program through grant 2006CB705800. P. Zhang

is supported by the special funds for Major State Research Projects through grant 2005CB321704.

References

- [1] I. Babuška, R. Tempone and G.E. Zouraris, Galerkin finite element approximations of stochastic elliptic partial differential equations, *SIAM J. Numer. Anal.* 42 (2004), 800-825.
- [2] I. Babuška, R. Tempone, G.E. Zouraris, Solving elliptic boundary value problems with uncertain coefficients by the finite element method: the stochastic formulation. *Comput. Methods Appl. Engrg.*, 194 (2005), 1251-1294.
- [3] I.S. Berezin and N.P. Zhidkov, *Computing Methods*, Pergamon Press, Oxford, 1965.
- [4] C. Canuto, M.Y. Hussaini, A. Quateroni and T.A. Zang, *Spectral Methods in Fluid Dynamics*, Springer-Verlag, New York, 1988.
- [5] M. Chen, A.A. Keller, D. Zhang, Z. Lu and G.A. Zyvoloski, A stochastic analysis of transient two-phase flow in heterogeneous porous media, *Water Resour. Res.*, 42 (2006), W03425.
- [6] M. Chen, D. Zhang, A. Keller and Z. Lu, A stochastic analysis of steady state two-phase flow in heterogeneous media, *Water Resour. Res.*, 41 (2005), W01006.
- [7] R. Courant and D. Hilbert, *Methods of Mathematical Physics*, Interscience Publication, New York, 1953.
- [8] G. Dagan, *Flow and Transport in Porous Formations*, Springer-Verlag, New York, 1989.
- [9] M.K. Deb, I. Babuška and J.T. Oden, Solution of stochastic partial differential equations using Galerkin finite element techniques, *Comput. Methods Appl. Mech. Engrg.*, 190 (2001), 6359-6372.
- [10] F. Delay, G. Porel and O. Banton, An approach to transport in heterogeneous porous media using the truncated temporal moment equations: Theory and numerical validation, *Transport in Porous Media*, 32 (1998), 199-232.
- [11] Y. Ding, *Applications and algorithms of SDEs*, Ph.D. Thesis in Peking University, 2007.
- [12] R. Ghanem and P. Spanos, *Stochastic Finite Element: A Spectral Approach*, Springer-Verlag, New York, 1991.
- [13] A. Guadagnini and S.P. Neuman, Recursive conditional moment equations for advective transport in randomly heterogeneous velocity fields, *Transport in Porous Media*, 42 (2001), 37-67.
- [14] E. Isaacson and H.B. Keller, *Analysis of Numerical Methods*, John Wiley and Sons, New York, 1966.
- [15] A. Keese, A review of recent developments in the numerical solution of stochastic partial differential equations (stochastic finite elements), *Institut für Wissenschaftliches Rechnen*, 2003.
- [16] M. Loève, *Probability Theory*, fourth ed., Springer, Berlin, 1978.
- [17] Z. Lu and D. Zhang, Accurate, effective quantification of uncertainty for flow in heterogeneous reservoirs using the KLME approach, *SPE Journal*, 12 (2006), 239-247.
- [18] L. Mathelin, M.Y. Hussaini and T.A. Zang, Stochastic approaches to uncertainty quantification in CFD simulations, *Numerical Algorithms*, 38 (2005), 209-236.
- [19] I.P. Mysovskih, Proof of the minimality of the number of nodes in the cubature formula for a hypersphere, *USSR Comput. Math. Math. Phys.*, 6 (1966), 15-27.
- [20] S.P. Neuman, Eulerian-Lagrangian theory of transport in space-time nonstationary velocity fields: Exact nonlocal formalism by conditional moments and weak approximations, *Water Resour. Res.*, 29 (1993), 633-646.

- [21] H. Niederreiter, *Random Number Generation and Quasi-Monte Carlo Methods*, SIAM, Philadelphia, Pennsylvania, 1992.
- [22] W.H. Press, S.A. Teukolsky, W.T. Vetterling and B.P. Flannery, *Numerical Recipes in C: The Art of Scientific Computing* (second edition), Cambridge University Press, Cambridge, 1995.
- [23] Y. Rubin, *Applied Stochastic Hydrogeology*, Oxford University Press, New York, 2003.
- [24] Ch. Schwab and R.A. Todor, Karhunen-Loève approximation of random fields by generalized fast multipole methods, *J. Comput. Phys.*, 217 (2006), 100-122.
- [25] A.H. Stroud, Remarks on the disposition of points in numerical integration formulas, *Mathematical Tables and Other Aids to Computation*, 11 (1957), 257-261.
- [26] M.A. Tatang, W. Pan, R.G. Prinn, G.J. McRae, An efficient method for parametric uncertainty analysis of numerical geophysical models, *J. Geophys. Res.*, 102 (1997), 925-21, 932.
- [27] R.A. Todor and Ch. Schwab, Convergence rates of sparse chaos approximations of elliptic problems with stochastic coefficients, *IMA J. Numer. Anal.*, to appear, 2007.
- [28] X. Wan and G. Karniadakis, Multi-element generalized polynomial chaos for arbitrary probability measures, *SIAM J. Sci. Comput.* 28 (2006), 901-928.
- [29] D. Xiu, Efficient collocational approach for parametric uncertainty analysis, *Commun. Comput. Phys.*, 2 (2007), 293-309.
- [30] D. Xiu and J.S. Hesthaven, High-order collocation methods for differential equations with random inputs, *SIAM J. Sci. Comput.*, 27 (2005), 1118-1139.
- [31] D. Xiu and G.E. Karniadakis, Modeling uncertainty in steady state diffusion problems via generalized polynomial chaos, *Comput. Methods Appl. Mech. Eng.*, 191 (2002), 4927-4948.
- [32] D. Xiu and G.E. Karniadakis, The Wiener-Askey polynomial chaos for stochastic differential equations, *SIAM J. Sci. Comput.*, 24 (2002), 619-644.
- [33] D. Xiu and G.E. Karniadakis, Modeling uncertainty in flow simulations via generalized polynomial chaos, *J. Comput. Phys.*, 187 (2003), 137-167.
- [34] D. Xiu and J. Shen, An efficient spectral method for acoustic scattering from rough surfaces, *Commun. Comput. Phys.*, 2 (2007), 54-72.
- [35] J. Yang, D. Zhang and Z. Lu, Stochastic analysis of saturated-unsaturated flow in heterogeneous media by combining Karhunen-Loève expansion and perturbation method, *J. Hydrology*, 294 (2004), 18-38.
- [36] D. Zhang, Nonstationary stochastic analysis of transient unsaturated flow in randomly heterogeneous media, *Water Resour. Res.*, 35 (1999), 1127-1141.
- [37] D. Zhang, *Stochastic Methods for Flow in Porous Media: Coping With Uncertainties*, Academic Press, San Diego, 2002.
- [38] D. Zhang and Z. Lu, An efficient, high-order perturbation approach for flow in random porous media via Karhunen-Loève and polynomial expansions, *J. Comput. Phys.*, 194 (2003), 773-794.